Draft version 0.0

ATLAS NOTE

March 26, 2015

# Searches for the exclusive double diffractive Higgs

L. Feremenga[a], L. Nodulman[b], C. C. Chau[c], S. Chekanov[b], J. Griffith[a], B. Blair[a]

[a] *University of Texas at Arlington*
[b] *Argonne National Laboratory*
[c] *University of Toronto*

## Abstract

# Contents

# 1 Introduction

Theoretical studies that attempt to estimate the event rates for the exclusive diffractive Higgs boson at the LHC have been previously preformed [1] [2]. In these studies rapidity gaps between the Higgs decay products and the outgoing protons play the most active role. At high luminosities however, these rapidity gaps are corrupted by pileup events and can hardly be used to separate exclusive processes from inclusive processes. This result has diverted attention to ATLAS' ALFA detectors which could be used as taggers for the outgoing protons. A search for an exclusive pion pair has been used to test the feasibility of these ALFA detectors [3].

The most recent experimental searches for exclusive events were done at 7 TeV by ATLAS and CMS [4] [5] [6]. Here isolated lepton pairs from QED production were searched for by looking for isolated vertices with only two lepton tracks; no rapidity gaps or proton tagging was used. At 8 TeV however the strategy of looking for vertices with only two tracks was found to be inefficient using exclusive $H \rightarrow W^+W^- \rightarrow l^+\nu l^-\nu$ Monte Carlo samples. Feasibility studies by the tracking group confirmed this inefficiency and demonstrated that vertexing algorithms at 8 TeV tend to generously associate tracks with vertices. This obviously contaminates the exclusive signal.

In this note a search for exclusive events using an algorithm that utilizes neither vertexing, rapidity gaps nor proton tagging is presented. Exclusive $H \rightarrow W^+W^- \rightarrow l^+\nu l^-\nu$ events survival rate is improved. The note is organized as follows: Section 2 describes briefly the physics of exclusive diffractive Higgs production. The Khoze Martin Ryskin (KMR) and CHIDe models are described and their sources of theoretical systematic uncertainties are outlined. A discussion of the Monte Carlo (MC) sample used to study the signal and a list of backgrounds and their MC is outlined as well in this section. Section 3 describes the object and event selection. Section 4 introduces the algorithm for selecting exclusive events. Here the signal survival rate is quoted and the exclusivity cut is tested in data. Section **??** estimates the expected number of signal events versus background events in the signal region.

# 2 Theory

The Feynman diagram shown in Figure 1 describes the production of the exclusive double diffractive Higgs boson. In this QCD mechanism two gluons interact through a top quark loop to form the Higgs boson while a third gluon is exchanged to keep the protons color neutral and hence intact. Calculations for this process have been studied extensively. The most popular calculations are performed by the KMR and the CHIDe models, which differ very slightly and predict similar cross sections [7][8]. Both models introduce the proton impact factor through the skewed unintegrated gluon density [9], calculate the probability of additional gluon density using the Sudakov form factor [10]. Both models also take into account the probability of soft interaction between the outgoing protons. This interaction tends to destroy the intactness of the outgoing protons, and hence destroys the rapidity gaps associated with exclusive processes. There are two main differences between the KMR and the CHIDe models: CHIDe uses different limits to compute the Sudakov factor and also includes an additional K-factor to introduce some NLO corrections. As a result, KMR predicts a higher cross section for the exclusive double diffractive Higgs than CHIDe. For a 125GeV Higgs KMR predicts 3 fb at $\sqrt{s}$ = 8TeV [7].

There are two main sources of theoretical systematic uncertainties that have to be studied: upper and lower Sudakov form factor scales, unintegrated gluon densities. Uncertainties associated with the rapidity gap survival probability were originally studied for the Tevatron and subsequently for the LHC [11]. In this analysis we will not use rapidity gaps for event selection so uncertainties from rapidity gaps are estimated to be minimal.

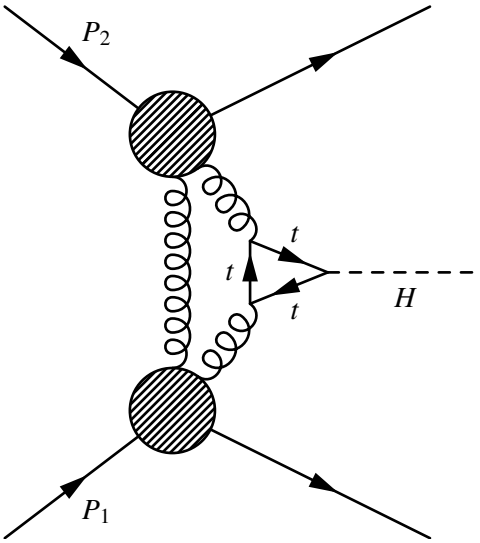


Figure 1:

## 2.1 Signal and Background Models

Both the KMR and CHIDe models are implemented in the Forward Physics Monte Carlo (FPMC). For signal we generate exclusive $H \to WW^* \to lvlv$ within KMR using FPMC and shower with Herwig. The results are then run through the full simulation of the ATLAS detector. This signal is characterized by very little activity around the dileptons.

Background processes can be separated into exclusive and inclusive. Inclusive backgrounds are those in which the two protons dissociate and the by-products are detected by the ATLAS detector. All these backgrounds are estimated using several MC samples except the W+jets background, in which the jet is misidentified as a lepton. A tested and verified data-driven method is used to estimate W+jets. See Section VIC from Ref. [12] for a detailed description of this method. The rest of the backgrounds are listed in Table 1.

The Z/$\gamma^*$+jets background is dominated by $Z/\gamma^* \to \tau\tau$+jets in which the taus decay leptonically to a different flavor channel. If the jets are misidentified as $E_{\mathrm{T}}^{\mathrm{miss}}$ the two leptons from the final state would fake the $H \to WW^* \to lvlv$ signature. Of the $Z/\gamma^* \to \tau\tau$+jets processes, the 0-jet process contributes the most signal contamination because it has the least activity around the dilepton system. These processes are generated with Alpgen and showered with Herwig.

$t\bar{t}$ is a background to the Higgs signature when the two top quarks decay to a WW system and a pair of b jets. MC@NLO is used to generate this process and Jimmy is used for showering. A single top quark is also a background process because a b jet can be misidentified as a lepton. Powheg is used to generate single top events and the showering is done with Pythia.

Because the signal is produced through gluon exchanges (See Figure 1), ggF Higgs is a background. ggF Higgs is generated with Powheg and showered with Pythia8. Apart from the intensity of activity about the dilepton system, the kinematics of ggF Higgs is identical to that of the exclusive Higgs.

Another irreducible inclusive background is a pair of W bosons. It is refered to as *inclusive WW* in this note. The final decay products are identical to signal so kinematic distributions are used to separate this background from signal. This is modelled by Powheg and Pythia.

The rest of the inclusive backgrounds will be referred in this note as *Other VV*. This is because they all constitute a pair of vector bosons. These are $W\gamma$, $W\gamma^*$, $Z\gamma$, $Z\gamma^*$, ZZ, WZ and double-parton interaction (DPI). The MC samples for these processes are listed in Table 1.

The main contribution to the exclusive background is the exclusive boson pair. Exclusive lepton pairs

have a very small cross section compared to exclusive boson pairs. Regardless, they are also considered in this study. In both cases photons are exchanged, in contrast to gluons exchanged in the exclusive Higgs production. Three diagrams contribute to the exclusive boson pairs. Figure **??** shows the three different diagrams. In a purely elastic process none of the two protons dissociate during the collision. The intact protons vanish along the beamline and the fiducial region sees only the WW decay products. In a Single Dissociative (SD) process one of the protons dissociate, but the remnants of the dissociation vanish along the beamline. A Double Dissociative (DD) process is similar to an inclusive process, but the proton remnants disappear along the beamline. The three processes have identical kinematic process, so it is impossible to distinguish them. Only the purely elastic diagram is modeled by the available MC, Herwig++. Data driven methods are used to estimate the SD and DD contributions.

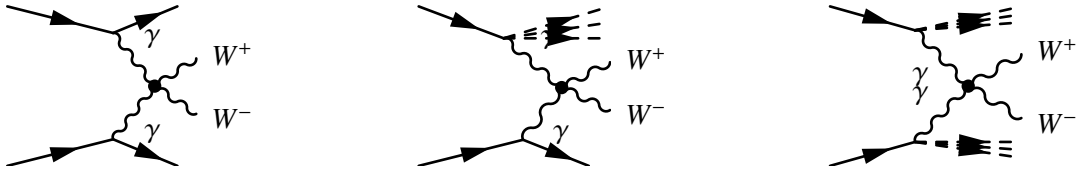


Figure 2: Diagrams that contribute to the exclusive WW processes. [Left] A purely elastice process. No proton dissociates and the two protons vanish along the beamline. [Middle] A single dissociative (SD) process. One proton dissociates but vanishes along the beamline. [Right] A double dissociative (DD) process. Both protons dissociate but the remnants vanish along the beamline. Rapidity gaps are present in all three diagrams and the kinematic distributions are identical, so they are indistinguishable.

| Inclusive Background | Exclusive Background |
|---|---|
| Drell Yan Z/$\gamma^*$+jets (Alpgen+Herwig) | WW (Herwig++) |
| W$\gamma$ +jets (Alpgen+Jimmy) | $l^+l^-$ (Herwig++) |
| WZ, WW, ZZ, ggF Higgs (Powheg+Pythia8) | |
| $t\bar{t}$ (MC@NLO+Jimmy) | |
| single top (AcerMC+Pythia) | |
| Z$\gamma$ +jets (Sherpa) | |

Table 1: Background samples used.

### 2.2 Data Samples

All the data used is from the ATLAS 2012 8 TeV run and sums up to a total integrated luminosity of 20.3 fb$^{-1}$. The D3PDs used are the most up-to-date and are identified with the tag p1328/p1329. The integrated luminosity is obtained through an ATLAS luminosity calculator [13].

## 3 Event and Object Selection

At preselection, events must pass an OR of `EF_e24vhi_medium1`, `EF_mu24i_tight`, `EF_e60_medium1`, `EF_mu36_tight`, `EF_e12Tvh_medium1_mu8`, `EF_mu18_tight_mu8_EFFS` and `EF_2e12Tvh_loose1` to get considered for analysis. They must also have exactly two leptons with $p_{\mathrm{T}} > 15$ GeV. A reconstructed primary vertex is not required to have a minimum number of tracks associated with it. All other preselection cuts are identical to those used for the $H \to WW^* \to \ell^+\ell^-$ study in Ref. [12].

The electron identification criteria closely follows the standard $H \to WW^* \to \ell^+\ell^-$ selection which relies on a likelihood-based method to identify electrons from electromagnetic (EM) showers and Inner Detector (ID) tracks. A more detailed description of this method can be found in Ref. [12]. EM showers and ID tracks are required to have $p_{\mathrm{T}} > 15$ GeVand lie in pseudorapidity less than 2.47 and out of the detector crack ( [1.37,1.52]). Electron candidates with $15 < p_{\mathrm{T}} < 25$ GeVhave to satisfy the very tight likelihood requirement and those with $p_{\mathrm{T}} > 25$ GeVhave to satisfy the medium likelihood requirement. This is because the latter are less likely to be misidentified objects. Calorimeter isolation is also imposed on electron objects by considering the energy deposited in a cone of $\Delta R = 0.3$ around the electron object cluster. Track isolation is also considered by taking the sum $p_{\mathrm{T}}$ of all the tracks with $p_{\mathrm{T}} > 400$ MeV within a cone of size $\Delta R = 0.3$. To separate these electron objects from prompt electrons, impact parameter variables are used.

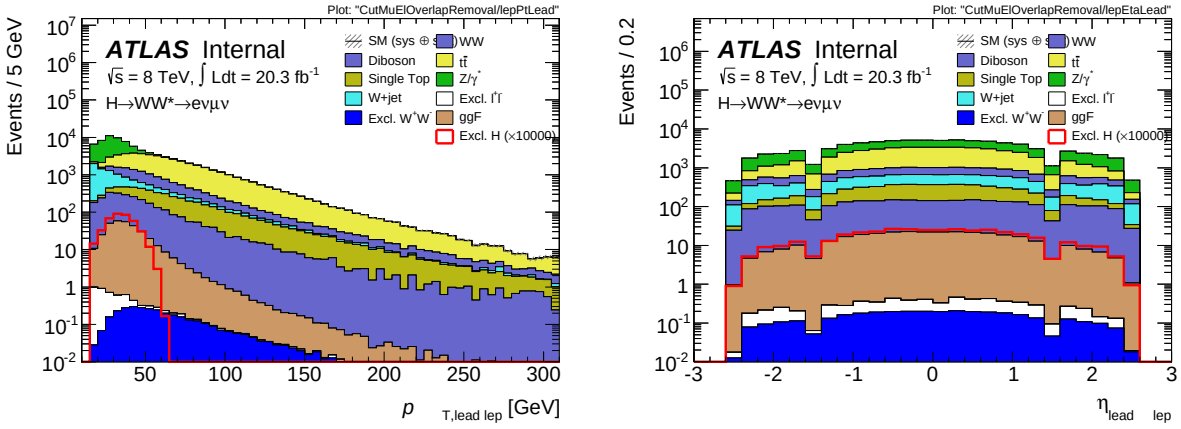


Figure 3: Electron distributions

Candidates for muon objects should be objects with matched hits from the ID and the Muon Spectrometer (MS). The algorithms that match ID tracks to MS tracks are described in detail in Ref. [14]. These objects are further required to have $p_{\mathrm{T}} > 15$ GeV and must lie within pseudorapidity of 2.47. The sum of the pixel hits and dead sensors should be at least 1. The sum of sct hits and dead sensors should also be at least 5.

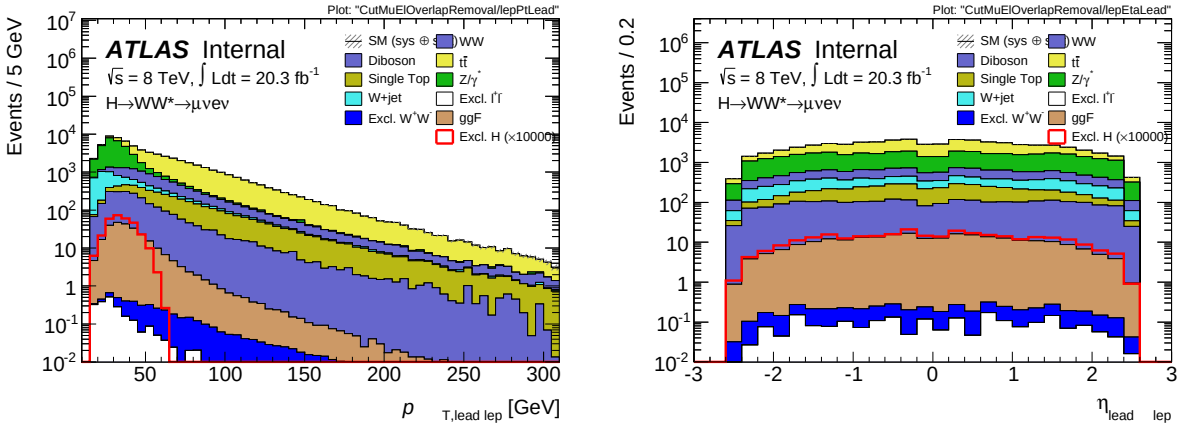


Figure 4: Muon distributions

Tracks are required to have at least 1 pixel hit and at least 4 sct hits and have at least 400 MeV $p_{\mathrm{T}}$. They are also required to be within $|\eta| < 2.47$.

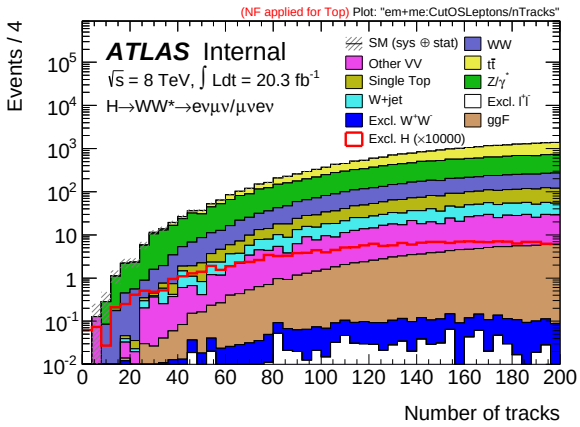


Figure 5: Number of selected tracks

The signal region for events that pass the pre-selection criteria is carefully designed to select events with Higgs properties. An exclusivity requirement is further imposed. The lepton with higher $p_{\mathrm{T}}$ is required to have $p_{\mathrm{T}} > 25$ GeV. This will be refered to as the 'leading lepton'. The second lepton, with lower $p_{\mathrm{T}}$ is required to have $p_{\mathrm{T}} > 15$ GeV. It will be refered to as the 'sub-leading lepton'. The high $p_{\mathrm{T}}$ selection on the leptons is meant to reduce W+jets and QCD multi-jets backgrounds, where low-$p_{\mathrm{T}}$ jets are mis-identified as leptons. To exploit the fact that the SM Higgs is neutral, the leading and sub-leading leptons are required to be of opposite sign. This cut will be refered to as 'OS Leptons' in this note.

The invariant mass of the dilepton system $m_{ll}$, is demanded to be fall within 10 GeV and 55 GeV. The reason for a lower bound is that some of the backgrounds such at Z+jets are not modelled correctly at low $m_{ll}$. In this analysis only Z+jets MC samples generated at $m_{ll} > 10$ GeV are used. Figure **??** shows the $m_{ll}$ distribution for events that pass the preselection cuts, lepton $p_{\mathrm{T}}$ cuts and the opposite sign requirement on the leptons. The $m_{ll} > 10$ GeV cut yields a signal survival efficiency of 98%. Figure **??** also justifies an upper bound on $m_{ll}$ for Higgs events. Since the Higgs boson is of spin zero, $m_{ll}$ tends to peak at lower values than for the WW backgrounds. A $m_{ll} < 55$ GeV cut rejects 75% of inclusive WW background and keeps 86% of signal.

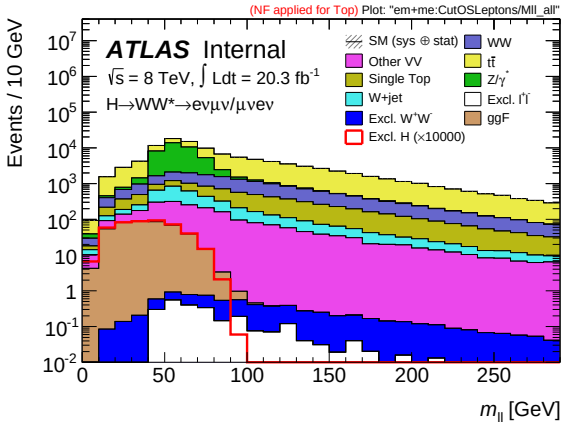


Figure 6: $m_{ll}$ distribution for signal (scaled by $10^4$) and relevant backgrounds for events that pass preselection, lepton $p_{\mathrm{T}}$, and OS lepton cuts. Z+jets are not well modelled for $m_{ll} < 10$ GeV, so we consider events with $m_{ll} > 10$ GeV. Signal survival after this cut is 98%. An $m_{ll} < 55$ GeV cut further rejects 75% of WW background while keeping 86% of signal.

The neutrinos in the signal final state are identified by a momentum imbalance in the detector. This imbalance is quantified by the variable 'missing transverse momentum', $E_{\mathrm{T}}^{\mathrm{miss}}$ that is calculated as

$$E_{\mathrm{T}}^{\mathrm{miss}} = -\left( \sum_{selected} p_{\mathrm{T}} + \sum_{soft} p_{\mathrm{T}} \right) \quad (1)$$

where $\sum_{selected} p_{\mathrm{T}}$ is the vectorial sum of $p_{\mathrm{T}}$ from all the objects identified by ATLAS identification algorithms, such as leptons, photons and jets. In this analysis these objects are required to have $p_{\mathrm{T}} > 20$ GeV. $\sum_{selected} p_{\mathrm{T}}$ is the vectorial sum of $p_{\mathrm{T}}$ from all other objects that have low values of $p_{\mathrm{T}}$, extracted from tracks with $p_{\mathrm{T}} > 0.5$ GeV that originate from the primary vertex. Both $E_{\mathrm{T}}^{\mathrm{miss}}$and its relative direction to leptons and jets are effective variables in rejecting Drell-Yan $\tau^+\tau^-$ background, where $E_{\mathrm{T}}^{\mathrm{miss}}$ aligns with a final state lepton. A special variable, $E_{\mathrm{T,rel}}^{\mathrm{miss}}$(see Ref. [12] for a more detailed description of this variable) is used to quantify how close in the transverse plane $E_{\mathrm{T}}^{\mathrm{miss}}$ is to leptons and jets:

$$E_{\mathrm{T,rel}}^{\mathrm{miss}} = \begin{cases} E_{\mathrm{T}}^{\mathrm{miss}} \sin \Delta\phi_{near} & \text{if } \Delta\phi_{near} < \pi/2 \\ E_{\mathrm{T}}^{\mathrm{miss}} & \text{otherwise,} \end{cases} \quad (2)$$

where $\Delta\phi_{near}$ is the azimuthal separation of the $E_{\mathrm{T}}^{\mathrm{miss}}$ and the nearest high-$p_{\mathrm{T}}$jet or lepton. Figure ... shows ...

show plot of METRel.... it should prove that Ztautau is reduced by cutting on it.

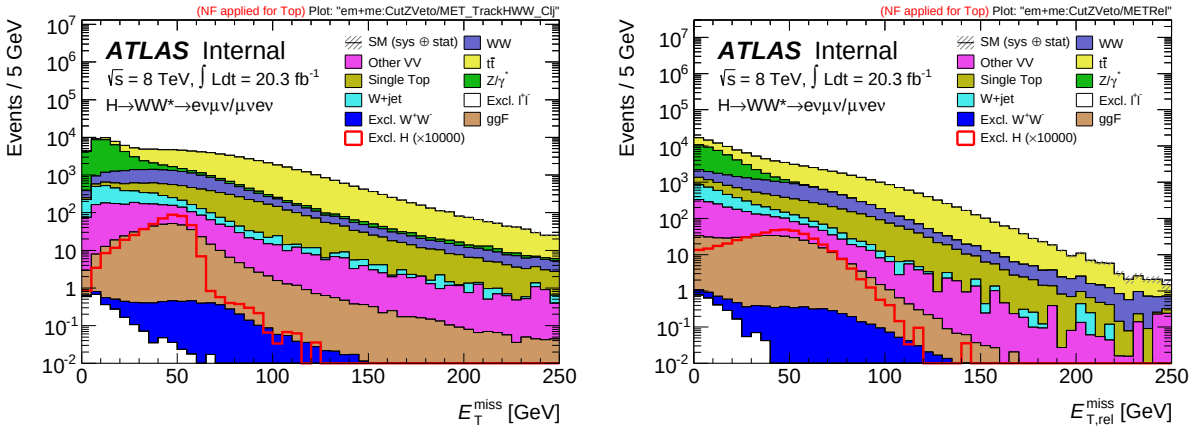


Figure 7: Talk about MET selection

talk about dphillmet and add a plot....
talk about ptll and add a plot ...
talk about dphill and add a plot

# 4 Exclusivity

With the high pileup environment in 8 TeV data it is crucial to improve on what has been done with 7 TeV data [4] [5] [6]. With 8 TeV data, the strategy adopted at 7 TeV of requiring a 2-track vertex and not having another track within 3 mm is only 30% efficient. This strategy is unreliable because the vertexing algorithms can be overly enthusiastic about associating tracks to a vertex. As a result, originally 2-track vertices are assigned 3 or more tracks.

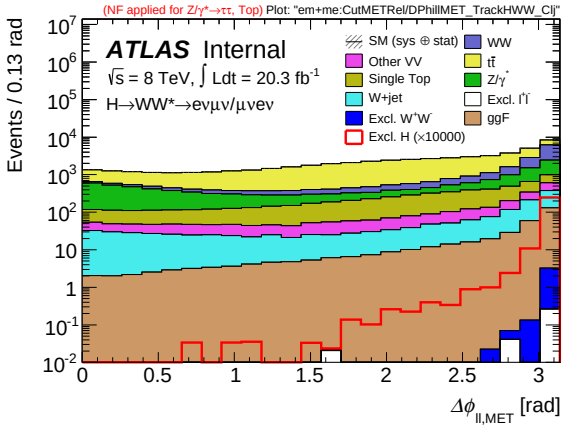


Figure 8: dphillmet

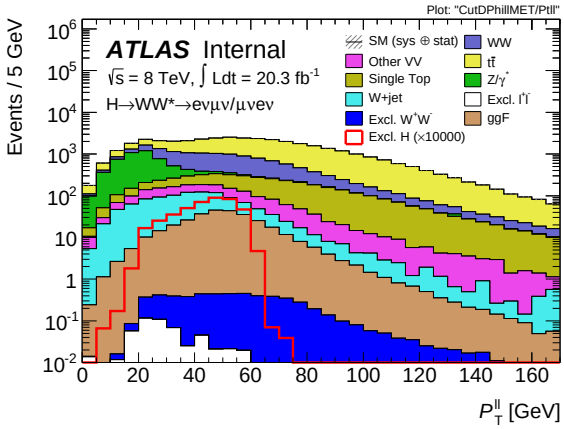


Figure 9: ptll

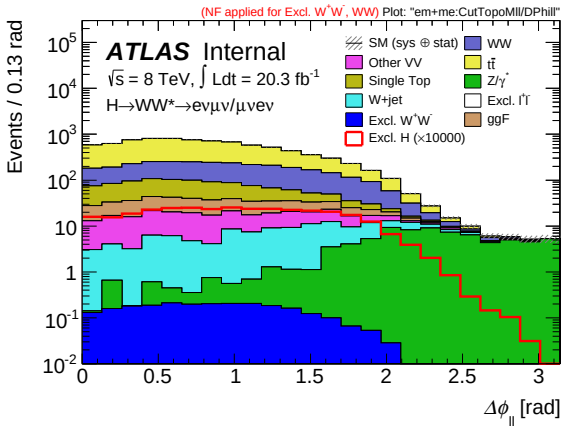


Figure 10: dphill

## 4.1 Strategy

The strategy used at 8 TeV is to demand that the lepton pair not have any tracks other than those from the two leptons within a window in $z_0$ along the beamline. Tracks are taken from the trk container and

| Cut | Excl. H | ggF H | $WW$ | Excl. $W^+W^-$ |
|---|---|---|---|---|
| Scale factors | NF = 100.00 | | | |
| blinding | 6.99 ± 0.05 | 585.63 ± 1.00 | 11641.95 ± 18.53 | 6.49 ± 0.03 |
| lepton $p_T$ 25, 15 GeV | 4.59 ± 0.04 | 434.84 ± 0.86 | 10657.89 ± 17.79 | 5.84 ± 0.03 |
| OS leptons | 4.59 ± 0.04 | 434.23 ± 0.86 | 10618.52 ± 17.76 | 5.82 ± 0.03 |
| $m_{\ell\ell} > 10$ GeV | 4.52 ± 0.04 | 430.02 ± 0.86 | 10606.74 ± 17.75 | 5.82 ± 0.03 |
| $E^{\text{miss}}_{\text{T,rel}} > 25$ GeV | 4.27 ± 0.04 | 358.80 ± 0.78 | 8494.57 ± 15.88 | 5.23 ± 0.03 |
| $\Delta\phi_{\ell\ell,MET} > 1.57$ | 4.27 ± 0.04 | 318.16 ± 0.74 | 7590.42 ± 15.01 | 5.22 ± 0.03 |
| $p_{T,\ell\ell} > 30$ GeV | 3.83 ± 0.04 | 285.01 ± 0.70 | 6183.69 ± 13.54 | 4.63 ± 0.03 |
| $m_{\ell\ell} < 55$ GeV | 3.28 ± 0.03 | 246.08 ± 0.65 | 1578.43 ± 6.80 | 0.81 ± 0.01 |
| $\Delta\phi_{\ell\ell} < 1.8$ | 2.98 ± 0.03 | 231.26 ± 0.63 | 1462.57 ± 6.54 | 0.77 ± 0.01 |
| Exclusivity Cuts | | | | |

Table 2: Yields are normalized to 20.3fb$^{-1}$. Define 'Blinding'

required to have at least 1 pixel hit and at least 4 sct hits. In contrast, lepton tracks are taken from the lepton containers. It is therefore necessary to match the lepton tracks to two tracks from the trk container. For a track in the trk container to be considered a match to a lepton track it is required to be within 0.01 in $\Delta R$ and within 1 mm in $z_0$, with respect to the beamline. The tracks in the electron or muon containers are obtained using algorithms (GSM) different from the algorithms used in the trk container. For this reason, a lepton track may not be matched to a track in the trk container or may be matched to multiple tracks in the trk container. Figure 11 shows the number of tracks from the trk container that match the leading lepton in the event. The distribution on the left is for matching tracks to an electron and that on the right is for matching tracks to muons.

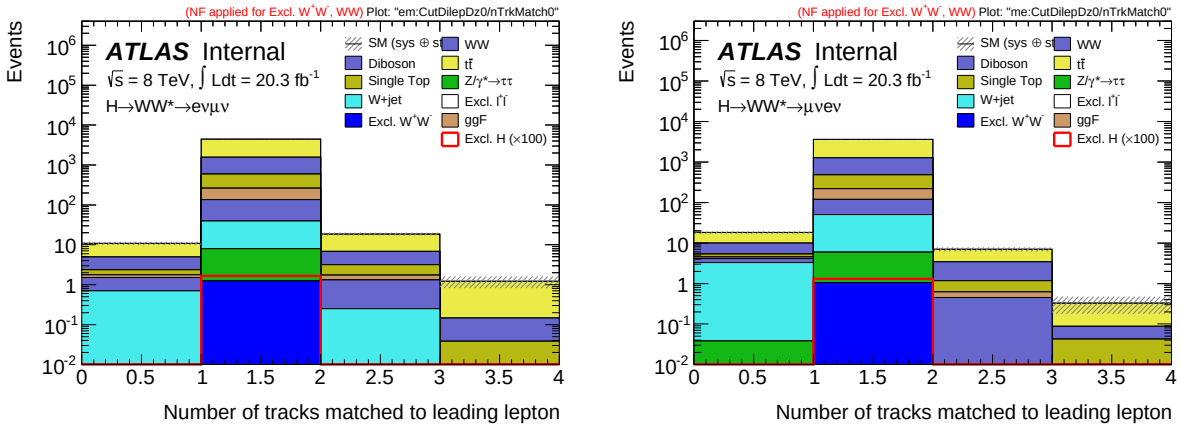


Figure 11: Number of tracks from the trk container that are matched to the leading lepton tracks. [Left] The leading lepton is an electron. [Right] The leading lepton is a muon.

Because electrons undergo bremsstrahlung more frequently than muons, there are more tracks matched to electrons than to muons. All the tracks matched to a lepton are therefore considered to be brehming from that lepton.

The exclusivity cut depends on how far in $z_0$ the closest unmatched track is from the lepton track pair. Figure 12 illustrates how this is quantified. The two lepton tracks are first required to be within 1 mm in $z_0$ to ensure that they indeed are from the lepton pair. The average $z_0$ position computed from the individual lepton track $z_0$'s is considered the dilepton vertex. The distance of the closest unmatched track $\Delta z_1$ is the

exclusivity variable that is cut on. Figure 13 shows $\Delta z_1$ for signal and several backgrounds. The signal is scaled by a factor of 100 to make it visible because it is heavily dominated by the backgrounds. The $\Delta z_1$ distribution in signal and other exclusive processes is characterized by a tail more spread out than in inclusive processes. Several values of $\Delta z_1$ were tried to maximize $signal/\sqrt{background}$. Figure 14 shows $signal/\sqrt{background}$ for four values of $\Delta z_1$. This analysis settles on $\Delta z_1 > 1mm$ as the optimal exclusivity cut.

Figure 12: Illustration of the exclusivity variables.

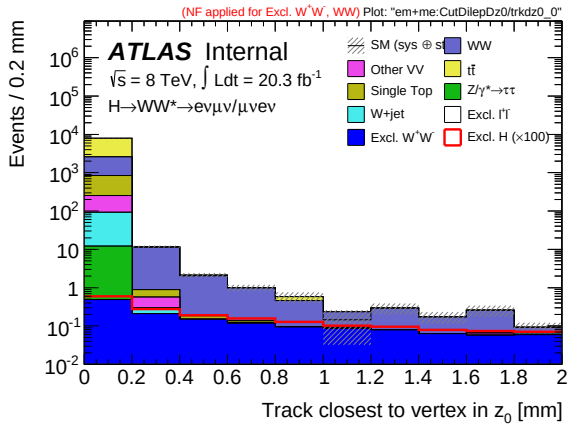


Figure 13: The main exclusivity variable $\Delta z_1$, which is the distance of the closest unmatched track to the dilepton vertex in $z_0$. Signal is scaled by 100. $\Delta z_1$ has a longer tail in exclusive processes compared to inclusive processes. This distrinction is exploited in this study.

## 4.2 Performance in data

A region in data that is rich in $Z \to \tau\tau$ events is used to validate the exclusivity selection criteria. This region follows the control region used in Ref. [12] to constrain $Z \to \tau\tau$+0-jets events in the $H \to WW^* \to \ell^+\ell^-$ study. In this study we apply it to any jet multiplicity. The selection is similar to the signal selection criteria except the following: $m_{ll}$ region is expanded to cover $10 < m_{ll} < 80$GeV, $p_T^{ll}$ is changed

$z_{av} = (z_1 + z_2)/2$

Extra Track

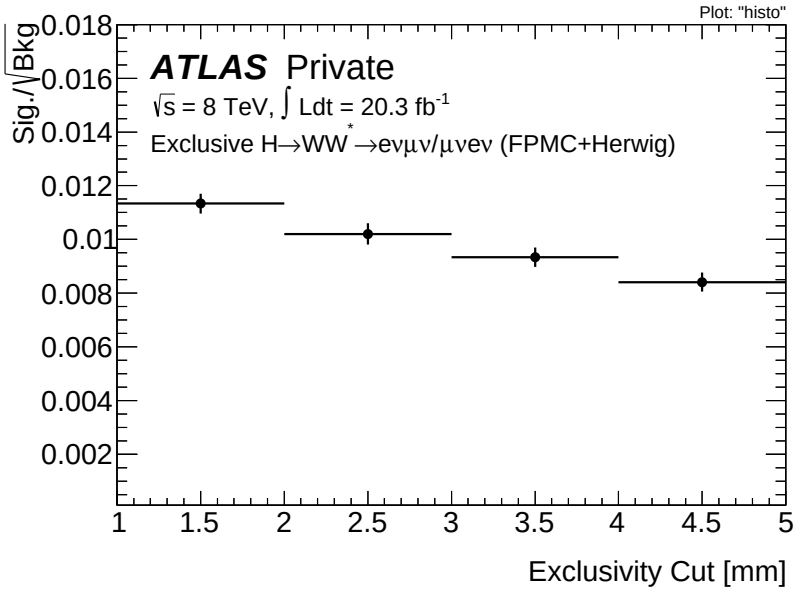


Figure 14: $signal/\sqrt{background}$ for 4 values of $\Delta z_1$. This analysis settles on $\Delta z_1 > 1mm$ as the optimal exclusivity cut.

| | $Z \to \mu\mu$ | $Z \to \tau\tau$ |
|---|---|---|
| Sherpa | 9.23 | |
| AlpgenPythia | 1.65 | |
| AlpgenJimmy | 4.36 | 4.72 |
| PowhegPythia | 2.35 | |

Table 3:

to $p_T^{ll} < 30$GeV. The $\Delta\phi_{ll}$ cut is also droppped. Figure 15 shows some kinematic distributions of events in this $Z \to \tau\tau$ region. This region achieves –% purity.

Figure **??** shows exclusivity variables ... talk about the mismodelling factor ....

$$\text{MC Exclusivity Correction Factor, MF} = \frac{N^{mc}_{after\ excl.}/N^{mc}_{before\ excl.}}{N^{data}_{after\ excl.}/N^{data}_{before\ excl.}} \tag{3}$$

comparison between MCs ...

# 5 Background Estimation

## 5.1 Exclusive WW

## 5.2 Inclusive WW

## 5.3 Other Backgrounds

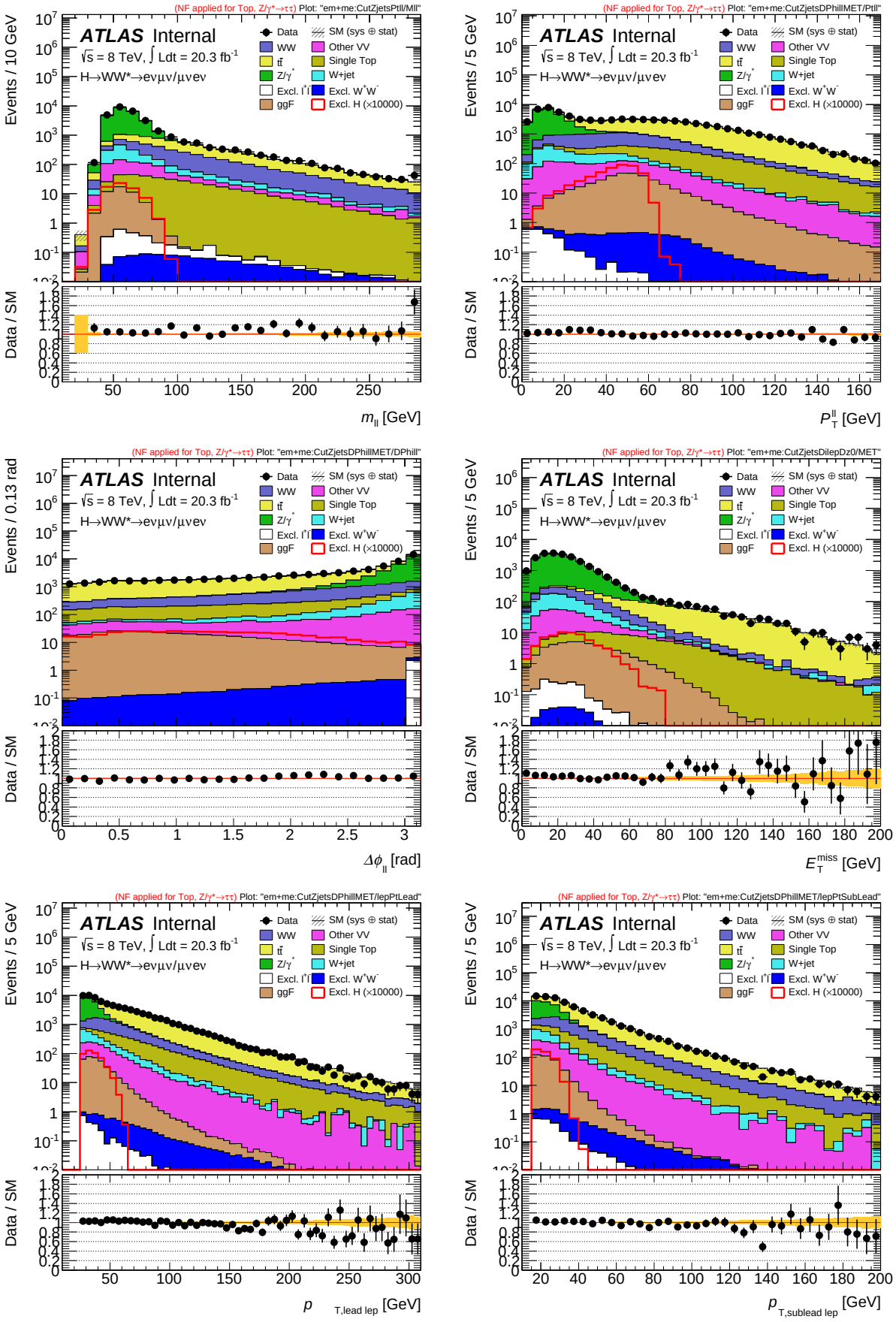


Figure 15: $Z \to \tau\tau$ CR

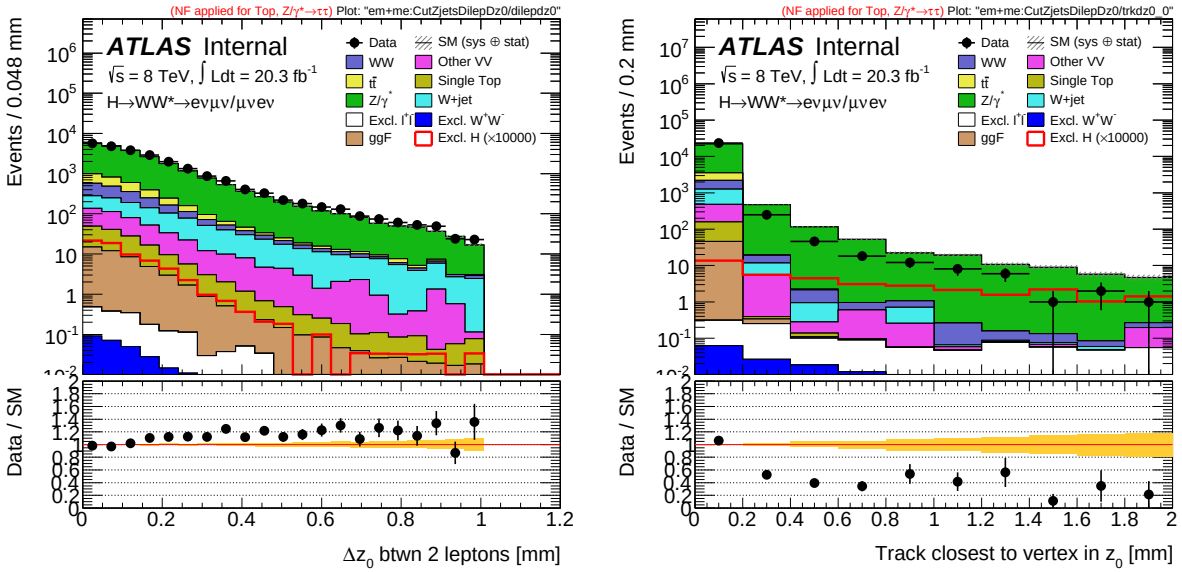


Figure 16: Exclusivity variables in the $Z \to \tau\tau$ CR

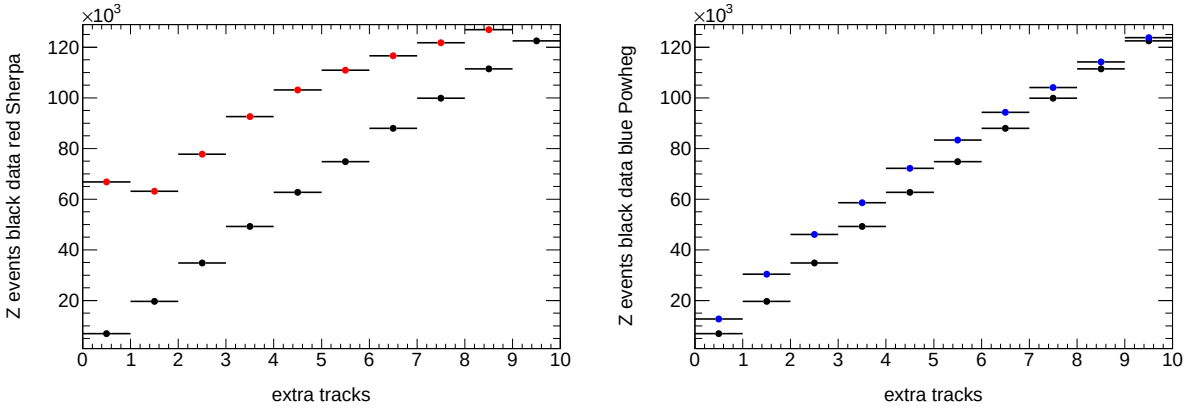


Figure 17: Number of extra tracks within a 1.5 mm window around the di-muon vertex.

# References


[1] V. A. Khoze, A. D. Martin, and M. Ryskin, *Higgs or dijet production in double rapidity gap events*, arXiv:hep-ph/0006005 [hep-ph].

[2] V. A. Khoze, A. D. Martin, and M. Ryskin, *Can the Higgs be seen in rapidity gap events at the Tevatron or the LHC?*, Eur.Phys.J. **C14** (2000) 525–534, arXiv:hep-ph/0002072 [hep-ph].

[3] R. Staszewski, P. Lebiedowicz, M. Trzebinski, J. Chwastowski, and A. Szczurek, *Exclusive $\pi^+\pi^-$ Production at the LHC with Forward Proton Tagging*, Acta Phys.Polon. **B42** (2011) 1861–1870, arXiv:1104.3568 [hep-ex].

[4] CMS, *Exclusive photon-photon production of muon pairs in $pp$ collisions at $\sqrt{s} = 7$ TeV*, JHEP **01** (2012) .

[5] CMS, *Search for exclusive or simi-exclusive photon pair production and observation of exclusive and semi-exclusive electron pair production in $pp$ collisions at $\sqrt{s} = 7$ TeV*, JHEP **11** (2012) .

[6] *Monte Carlo studies of two-photon production of muon pairs*, Tech. Rep. ATL-COM-PHYS-2013-1479, October, 2013.

[7] V. Khoze, A. Martin, and M. Ryskin, *Prospects for new physics observations in diffractive processes at the LHC and Tevatron*, Eur.Phys.J. **C23** (2002) 311–327, arXiv:hep-ph/0111078 [hep-ph].

[8] J. Cudell, A. Dechambre, O. Hernandez, and I. Ivanov, *Central exclusive production of dijets at hadronic colliders*, Eur.Phys.J. **C61** (2009) 369–390, arXiv:0807.0600 [hep-ph].

[9] A. D. Martin and M. Ryskin, *Unintegrated generalized parton distributions*, Phys.Rev. **D64** (2001) 094017, arXiv:hep-ph/0107149 [hep-ph].

[10] Y. Dokshitzer, D. Dyakonov, and S. Troyan, *Hard processes in quantum chromodynamics*, Physics Reports **58** (1980) no. 5, 269 – 395.

[11] V. A. Khoze, A. D. Martin, and M. Ryskin, *Soft diffraction and the elastic slope at Tevatron and LHC energies: A MultiPomeron approach*, Eur.Phys.J. **C18** (2000) 167–179, arXiv:hep-ph/0007359 [hep-ph].

[12] *Observation and measurement of Higgs boson decays to $WW^*$ with ATLAS at the LHC*, Tech. Rep. ATLAS-CONF-2014-060, CERN, Geneva, Oct, 2014.

[13] A. Collaboration, *https://atlas-lumicalc.cern.ch/*, .

[14] ATLAS Collaboration, G. Aad et al., *Measurement of the muon reconstruction performance of the ATLAS detector using 2011 and 2012 LHC proton-proton collision data*, Eur.Phys.J. **C74** (2014) no. 11, 3130, arXiv:1407.3935 [hep-ex].